CHEMISTRY OF MATERIALS
Article

Chem. Mater. **2009,** *21,* 4977–4983 4977
DOI:10.1021/cm902357m

Honeycomb-Patterned Hybrid Films and Their Template Applications via A Tunable Amphiphilic Block Polymer/Inorganic Precursor System

Lei Li,*[,†] Yawen Zhong,[†] Chunyin Ma,[‡] Jian Li,[†] Caikang Chen,[†] Aijuan Zhang,[†] Dingliang Tang,[‡] Suyuan Xie,[‡] and Zhi Ma*[,§]

[†]*College of Materials and* [‡]*College of Chemistry and Chemical Engineering, Xiamen University, Xiamen 361005, P. R. China, and* [§]*Shanghai Institute of Organic Chemistry, Chinese Academy of Sciences, Shanghai 200032, P. R. China*

Received July 31, 2009. Revised Manuscript Received September 11, 2009

Here, we show a facile and versatile method to prepare highly ordered inorganic patterns on solid substrates by pyrolyzing UV cross-linked polymer/functional precursor hybrid films. The cross-linked polymer matrix acted as structure-directing agent in a pyrolyzing process, whereas the functional precursor was converted into the skeleton of the micropatterns. The inorganic micropatterns could be further catalytically functionalized to grow CNT and ZnO nanorod arrays by simply changing different functional precursors. This simple technique offers new prospects in the field of micropatterns, nanolithography, and template.

Introduction

Patterning is of paramount importance in many areas of modern science and technology, with applications including the production of integrated circuits, information storage devices, miniaturized sensors, micro fluids devices, biochips, photonic bandgap crystals, micro-optical components, and diffractive optical elements.[1] However, it remains a challenge to achieve patterns in the synthetic world. The development of morphology- and size-controlled synthetic techniques in the field becomes an important theme of the modern material science. A variety of methods including breath-figure (BF) method,[2,3] colloidal particles array,[4] and lithographic techniques[5] have been developed to create ordered structures with micrometer and submicrometer dimensions. Especially, BF process is the most promising strategy for the fabrication of large size patterns having an ordered two-dimensional (2D) array of holes. The principle of this method is described as follows. The evaporation of volatile solvent can decrease the solution surface temperature, which causes water droplets to condense onto the solution surface under conditions of high humidity. Influenced by the surface convection and capillary attractive force, the condensed water droplets self-organize into a hexagonal array before their coagulation with each other. With continuing solvent evaporation, the polymer solidifies, and molds around the water droplets, acting as sacrificial template. After the solvent and water evaporate completely, honeycomb patterned pores are left on the film surface. The simple method offers new prospects in the field of microporous films,[6,7] as well as other technical advantages of low-cost and large area applicability.

One crucial point that has to be addressed for the practical application of the polymer honeycomb films is their thermal stability and organic solvent resistance in the harsh environments. There have been widespread efforts to utilize hybridization of organic polymer with inorganic structures instead.[8] It was already proposed by Bunz et al. that an organometallic conjugated polymer precursor was shaped into hexagonal array and then pyrolyzed to microstructured Si−C−Co ceramic. Also, a sol−gel process induced by soaking a microporous

*To whom correspondence should be addressed. Tel: +86-592-2186296. Fax: +86-592-2183937. E-mail: lilei@xmu.edu.cn.

(1) Geissler, M.; Xia, Y. N. *Adv. Mater.* **2004**, *16*, 1249.
(2) Bunz, U. H. F. *Adv. Mater.* **2006**, *18*, 973.
(3) (a) Stenzel, M. H.; Barner-Kowollik, C.; Davis, T. P. *J. Polym. Sci., Part A* **2006**, *44*, 2363. (b) Hayakawa, T.; Horiuchi, S. *Angew. Chem., Int. Ed.* **2003**, *42*, 2285. (c) Zhang, Y.; Wang, C. *Adv. Mater.* **2007**, *19*, 913. (d) Connal, L. A.; Vestberg, R.; Hawker, C. J.; Qiao, G. G. *Adv. Funct. Mater.* **2008**, *18*, 3706.
(4) (a) Li, Y.; Sasaki, T.; Shimizu, Y.; Koshizaki, N. *Small* **2008**, *4*, 2286. (b) Li, Y.; Lee, E. J.; Cai, W.; Kim, K. Y.; Cho, S. O. *ACS Nano* **2008**, *2*, 1108. (c) Chen, X.; Chen, Z. M.; Fu, N.; Lu, G.; Yang, B. *Adv. Mater.* **2003**, *15*, 1413. (d) Chen, X.; Sun, Z. Q.; Zheng, L. L.; Chen, Z. M.; Wang, Y. F.; Fu, N.; Zhang, K.; Yan, X.; Liu, H.; Jiang, L.; Yang, B. *Adv. Mater.* **2004**, *16*, 1632.
(5) (a) George, M. C.; Nelson, E. C.; Rogers, J. A.; Braun, P. V. *Angew. Chem., Int. Ed.* **2009**, *48*, 144. (b) Lee, J. Y.; Yin, D. H.; Horiuchi, S. *Chem. Mater.* **2005**, *17*, 5498. (c) Horiuchi, S.; Fujita, T.; Hayakawa, T.; Nakao, Y. *Adv. Mater.* **2003**, *15*, 1449. (d) Yao, J. M.; Yan, X.; Lu, G.; Zhang, K.; Chen, X.; Jiang, L.; Yang, B. *Adv. Mater.* **2004**, *16*, 81.
(6) (a) Lu, Y.; Ren, Y.; Wang, L.; Wang, X. D.; Li, C. X. *Polymer* **2009**, *50*, 2035. (b) Barner-Kowollik, C.; Dalton, H.; Davis, T. P.; Stenzel, M. H. *Angew. Chem., Int. Ed.* **2003**, *42*, 3664.
(7) (a) Böker, A.; Lin, Y.; Chiapperini, K.; Horowitz, R.; Thompson, M.; Carreon, V.; Xu, T.; Abetz, C.; Skaff, H.; Dinsmore, A. D.; Emrick, T.; Russell, T. P. *Nat. Mater.* **2004**, *3*, 302. (b) De Boer, B.; Stalmach, U.; Nijland, H.; Hadziioannou, G. *Adv. Mater.* **2000**, *12*, 1581.
(8) (a) Karthaus, O.; Cieren, X.; Maruyama, N.; Shimomura, M. *Mater. Sci. Eng., C* **1999**, *10*, 103. (b) Zhang, K.; Zhang, L. W.; Chen, Y. M. *Macromol. Rapid Commun.* **2007**, *28*, 2024. (c) Englert, B. C.; Scholz, S.; Leech, P. J.; Srinivasarao, M.; Bunz, U. H. F. *Chem.—Eur. J.* **2005**, *11*, 995.

Published on Web 09/30/2009

polymer film bearing anhydrides groups into 3-aminopropyltrimethoxysilane (APTES) created silica porous film. However, the applicability of the mentioned process is limited by the particular chemical reaction and time-consuming synthesis. A versatile preparation of hybrid honeycomb structures and resultantly catalytically active or otherwise functional microstructured films are more desirable.

In this article, we report the facile fabrication of robust inorganic micropatterns into hexagonally ordered arrays by pyrolyzing the photochemically cross-linked honeycomb shaped polymer/functional precursor hybrid films, prepared by a BF process. Pyrolysis decomposes the polymer matrix and converts the incorporated functional precursor into the skeleton of micropatterns simultaneously. We demonstrate the generality of the method by forming ordered structures with different chemical species as well as on various substrates, simply through the choice of functional precursors. Particularly, the resultant micropatterns are catalytically active, which can grow aligned carbon nanotubes (CNTs) and zinc oxide (ZnO) nanorods, probably the most important nanomaterials in today's research,[9,10] on rigid substrate with a honeycomb structure.

Experimental Section

Materials. APTES was purchased from Acros Chemical Company. Ferrocene, zinc acetylacetonate ($Zn(acct)_2$) and carbon disulfide (CS_2) were purchased from Shanghai Chemical Reagent Plant. All the chemical reagents were used without further purification. The glass substrates were cleaned by detergent and acetone successively and air-dried. Silicon wafers were used as received.

The preparation of amphiphilic diblock copolymer, polystyrene-*b*-poly(acrylic acid) (PSPAA), was synthesized via atom-transfer radical polymerization with a similar procedure as reported in ref 11. The relative molecular weights of PS and PAA blocks were 9000 and 2500 g mol^{-1}, respectively. The molecular weight distribution (M_w/M_n) of such diblock copolymer was 1.07. The relative molecular weights and M_w/M_n were measured by a Waters gel permeation chromatography (GPC) system equipped with a Waters 1515 Isocratic HPLC pump, a Waters 2414 refractive index detector (RI), a Waters 2487 dual λ absorbance detector (UV) and a set of Waters Styragel columns (HR3, HR4 and HR5, 7.8 × 300 mm). GPC measurements were carried out at 35 °C using tetrahydrofuran (THF) as an eluent with a flow rate of 1.0 mL/min. The system was calibrated with polystyrene standards.

Preparation of Honeycomb Structured Films. The static breath-figure process was operated in a 25 mL straight-mouth glass bottle with a cap. A saturated relative humidity in the vessel was achieved by adding 2 mL of distilled water into the bottle beforehand. A piece of substrate was adhered onto the top of a plastic stand with double-sided tape and placed into the glass vessel. The substrate was 1 cm higher than the liquid level. Polymer and functional precursor were mixed with a fixed weight ratio (3/1, w/w) and dissolved in CS_2. The solution concentration was 15 mg mL^{-1}. The honeycomb film was prepared by casting 100 μL of solution onto the substrate with a microsyringe. With organic solvent volatilization, the transparent solution became turbid. The film was taken out for microscope observation after complete solvent evaporation. All the experiments were carried out at room temperature unless stated otherwise.

Photochemical Cross-Linking and Pyrolyzing. The photochemical cross-linking was performed at 30 °C in a UVO cleaner ZWLH-5 (Tianjin, China) at the presence of air, by exposing the polymer thin films into UV light. The cleaner generated UV emissions at a wavelength of 254 nm and power of 500 W. The distance between the UV source and the film surface was 10 cm. After 4 h UV exposure, the cross-linked film was heated to 450 °C within 2 h and held for another 5 h under air atmosphere. During the pyrolysis, the functional precursor turned into oxide and replaced the polymer skeleton eventually. Inorganic patterns with various chemical species were prepared simply by choosing different functional precursors.

Preparation of Silica Patterns. Highly ordered silica patterns on glass substrate were fabricated by choosing APTES as the silica precursor after the mentioned procedures.

Preparation of Carbon Nanotube Arrays. Catalytically active ferrous patterns were formed by choosing ferrocene as functional precursor after the mentioned procedures. The aligned CNTs with a honeycomb structure were synthesized by thermal chemical vapor deposition (CVD) in a 30 mm diameter quartz tube furnace. The obtained ferrous micropatterned on silicon wafer worked as the catalytic iron film without further treatment. An Ar/H_2 gas mixture (25% H_2) was used as the buffer gas and pure acetylene served as the carbon source. Typically, the growth of CNT was carried out at 750 °C with 100 sccm acetylene and 500 sccm Ar + 25% H_2 for 15 min.

Preparation of the ZnO Nanorod Arrays. Honeycomb structured ZnO nanorod arrays were prepared by choosing $Zn(acct)_2$ as functional precursor after the mentioned procedures with a sequent hydrothermal process. Hydrothermal ZnO growth was carried out by suspending a piece of solid substrate (silicon or glass) having micropatterned ZnO upside-down in an open crystallizing dish filled with an aqueous solution of zinc nitrate hydrate (0.025m) and methenamine or diethylenetriamine (0.025m) at 90 °C. Reaction time spanned from 0.5 to 9 h. The substrate was then fished out, rinsed with deionized water, and dried.

Characterization and Apparatus. Scanning electronic microscopy (SEM) images were obtained using a Hitachi S4800 scanning electron microscope. A 10 KeV electron beam was used for the observation with a working distance of 10 mm in order to obtain secondary electron images. Atomic force microscopy (AFM) measurements were carried out in the tapping mode with a Seiko Instruments SPA400. We used silicon tips with a spring constant of 20 N/m. X-ray photoelectron spectroscopy (XPS) spectra were acquired with a PHI Quantum 2000 spectrometer using monochromated X-rays from an $Al_{K\alpha}$ source with a takeoff angle of 45° from the surface plane. The atomic fractions of carbon and oxygen were computed using the attenuation factors provided by the supplier and the sum of these atomic fractions was normalized to unity. Thermogravimetric (TG) analysis was taken on a Netzsch STA 409 EP Thermal Analyzer. The sample was heated from 25 to 450 °C at a rate of 5 °C/min and held for 5 h under air. The morphology and structure of the carbon nanotubes were characterized by high-resolution transmission electron microscopy (TEM, TECNAI F-30) with an acceleration voltage

(9) (a) Yan, Y. H.; Chan-Park, M. B.; Zhang, Q. *Small* **2007**, *3*, 24. (b) Avouris, P.; Freitag, M.; Perebeinos, V. *Nat. Photonics* **2008**, *2*, 341. (c) Kauffman, D. R.; Star, A. *Angew. Chem., Int. Ed.* **2008**, *47*, 6550.
(10) (a) Djurisic, A. B.; Leung, Y. H. *Small* **2006**, *2*, 944. (b) Ozgur, U.; Alivov, Y. I.; Liu, C.; Teke, A.; Reshchikov, M. A.; Dogan, S.; Avrutin, V.; Cho, S. J.; Morkoc, H. *J. Appl. Phys.* **2005**, *98*, 041301.
(11) Kang, Y. J.; Taton, T. A. *Angew. Chem., Int. Ed.* **2005**, *44*, 409.

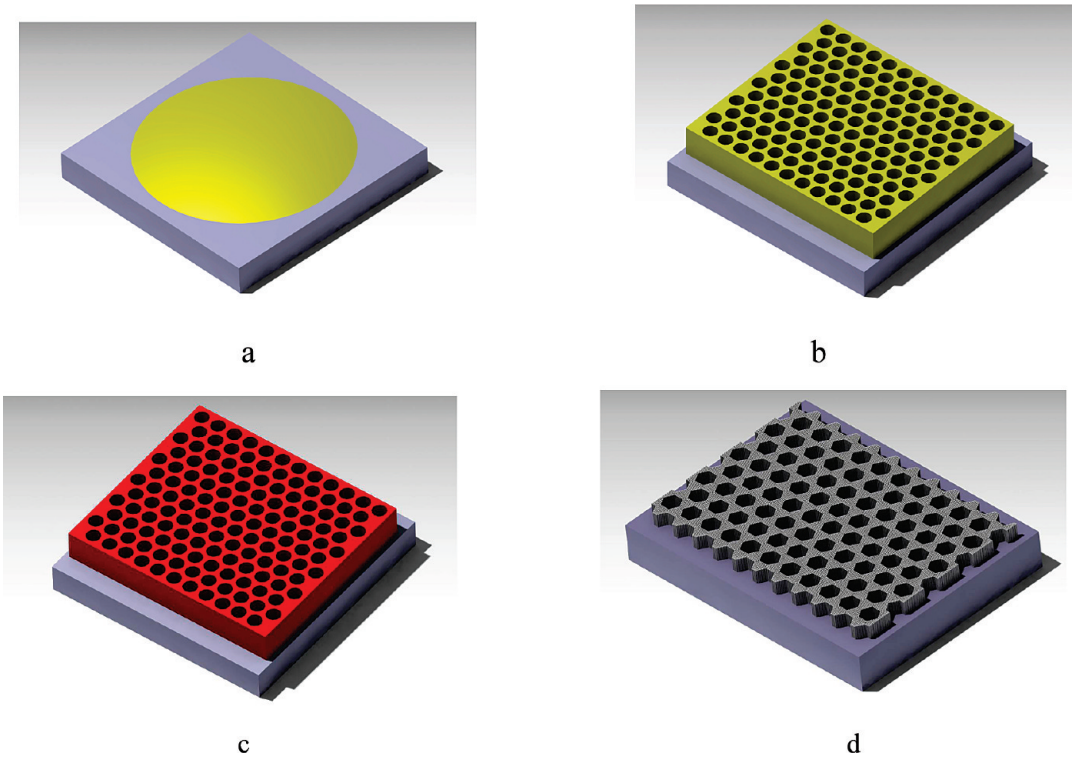

Figure 1. Schematic pictures of fabrication of inorganic micropatterns on substrate. (a) A droplet of diblock copolymer/functional precursor solution was casted on substrate by a microsyringe. (b) Highly regularly microstructured polymer film was formed on substrate after total evaporation of solvent under high humidity. (c) Polymer matrix was cross-linked and the honeycomb structures were preserved after photochemical process. (d) Inorganic micropatterns on substrate were formed after pyrolysis.

of 300 kV. The TEM specimens were prepared by dispersing the CNTs in ethanol. A drop of the suspension was deposited on a carbon-film-coated copper grid.

Results and Discussion

The fabrication process of robust inorganic micropatterns on substrate is schematically shown in Figure 1. First, a mixture of diblock copolymer/functional precursor was dissolved in CS_2. Then the solution was casted on substrate by a microsyringe (Figure 1a). After evaporation of solvent in saturated relative humidity, a highly regularly microstructured hybrid film was formed (Figure 1b). In the following UV irradiation, not only the polymer matrix was effectively cross-linked with improved thermal stability but also the honeycomb structures were well preserved (Figure 1c). The cross-linked polymer matrix acted as structure-directing agent in a sequent pyrolyzing process, whereas the functional precursor was converted into the skeleton of the micropatterns. Eventually, robust inorganic micropatterns were formed on the substrate after completely decomposing the polymer matrix (Figure 1d).

Although a variety of polymers have been used to prepare honeycomb structured films by BF method, the pattern forming mechanism is not yet well understood. The process has many variables, including the polymer chemical nature and structure, choice of organic solvent and surface, temperature, airflow velocity, and humidity level. Different polymers require different preparation conditions, which makes the process more empirical. Block copolymers and polymers with polar end groups are believed to be good candidates to prepare porous films by BF method because of their high segment density, which could effectively stabilize water droplets in BF method.[2,3] Various types of polymers have been employed to fabricate honeycomb-patterned films with controlled pore size, ranging from hundreds of nanometers to hundreds of micrometers.[12] Quite recently, we reported a static BF process to fabricate ordered microstructured polymer films. An amphiphilic diblock copolymer, PSPAA, was found forming regularly microporous structures in a wide solution concentration range by casting from $CHCl_3$.[13] Because the saturated relative humidity is achieved beforehand without the need of flow gas in static process, any uncertainties caused by flow disturbing are minimized. In fact, the static BF process is a robust method to fabricate ordered polymer films, which tolerates more variabilities in casting conditions, including molecular weight, temperature, and solution concentration. Microporous polymer films having the identical surface features are repeatable in each batch.[13−15] Herein, a similar BF process by casting

(12) (a) Englert, B. C.; Scholz, S.; Leech, P. J.; Srinivasarao, M.; Bunz, U. H. F. *Chem.—Eur. J.* **2005**, *11*, 995. (b) Connal, L. A.; Qiao, G. G. *Adv. Mater.* **2006**, *18*, 3024. (c) Tian, Y.; Liu, S.; Ding, H.; Wang, L.; Liu, B.; Shi, Y. *Polymer* **2007**, *48*, 2338. (d) Hayakawa, T.; Horiuchi, S. *Angew. Chem., Int. Ed.* **2003**, *42*, 2285.
(13) Li, L.; Chen, C. K.; Zhang, A. J.; Liu, X. Y.; Cui, K.; Huang, J.; Ma, Z.; Han, Z. H. *J. Colloid Interface Sci.* **2009**, *331*, 446.
(14) Li, L.; Chen, C. K.; Li, J.; Zhang, A. J.; Liu, X. Y.; Xu, B.; Gao, S. B.; Jin, G. H.; Ma, Z. *J. Mater. Chem.* **2009**, *19*, 2789.
(15) Li, L.; Zhong, Y. W.; Li, J.; Chen, C. K.; Zhang, A. J.; Xu, J.; Ma, Z. *J. Mater. Chem.* **2009**, *19*, No. DOI: 10.1039/b911714h.

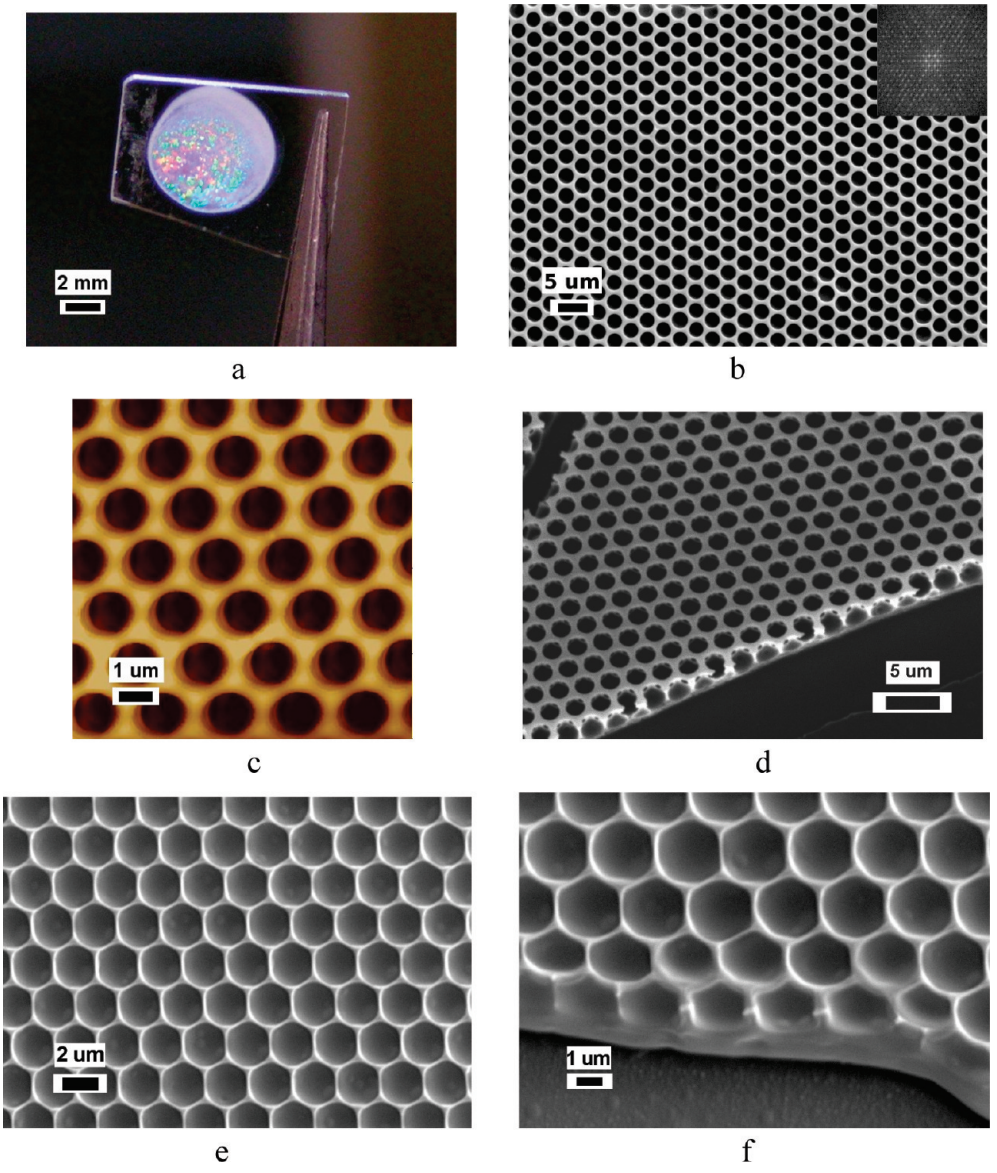

Figure 2. (a) Photograph of sunlight diffraction obtained from a honeycomb structured PSPAA/APETS film on glass substrate. (b) SEM and (c) topographic images of the honeycomb structured PSPAA/APTES film. (d) Cross-section view of honeycomb structured PSPAA/APETS film. (e) SEM image of honeycomb structured PSPAA/APETS film after 4 h UV irradiation. (f) Cross-section view of honeycomb structured PSPAA/APETS film after 4 h UV irradiation.

a PSPAA/functional precursor solution is employed to fabricate microporous hybrid films.

Figure 2a is the photograph of glass sheet, on which a structured hybrid film of PSPAA/APTES has formed. As expected from the highly ordered structures, the film exhibits an interesting nacre color because of sunlight diffraction and interference effects.[16] More precise microscopy studies by SEM and AFM are shown in images b and c in Figure 2, respectively (a SEM image in larger scan area is shown in the Supporting Information, Figure S1). It is clear that the film surface is made up by layer of highly ordered honeycomb structures with identical size. The associated fast Fourier transform (FFT) of the SEM image (the inset in Figure 2b), with first- and high-order spots, demonstrates the very regular character of the main structures. Though a large amount of APTES is incorporated into polymer matrix, no macrophase separation is observed in the whole film. This is ascribed to the strong hydrogen-bond interaction between the carboxyl groups of PAA and the amino group of APTES.[17] For more detailed insight into the geometry, we show the considerably magnified AFM height image in Figure 2c. The cross-section line scan profile gives the microporous thin film pore diameter, hole depth, and average pore separation as 1.2, 0.4, and 2.5 μm, respectively. Either top or cross-sectional view (Figure 2d) reveals that the resultant film has a monolayer of independent pores on dense polymer stratum without network structures.

The obtained honeycomb structures began to melt and collapsed upon heating up to 100 °C (the glass transition

(16) Billon, L.; Manguian, M.; Pellerin, V.; Joubert, M.; Eterradossi, O.; Garay, H. *Macromolecules* **2009**, *42*, 345.

(17) Brinke, G.; Ruokolainen, J.; Ikkala, O. *Adv. Polym. Sci.* **2007**, *207*, 113.

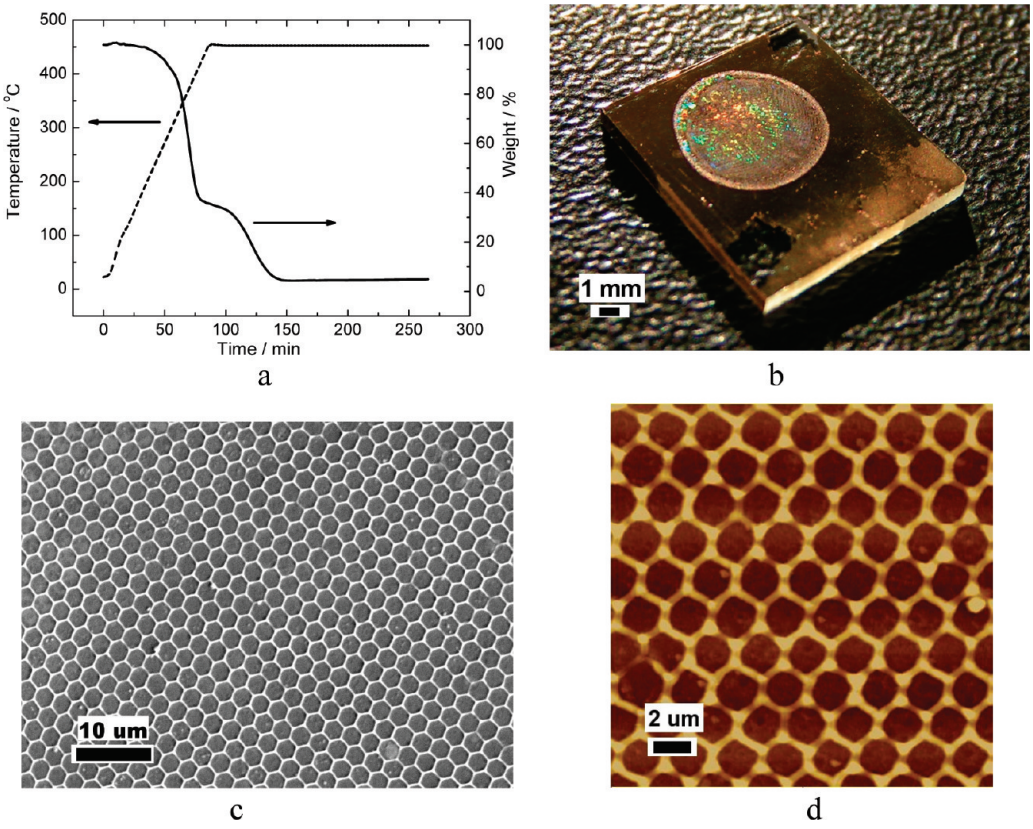

Figure 3. (a) Thermalgravity analysis of PSPAA after 4 h UV irradiation. (b) Photograph of sunlight diffraction obtained from a honeycomb structured silica patterns on glass substrate after pyrolysis. (c) SEM and (d) topographic images of the honeycomb structured silica pattern.

temperature, T_g, of the PS matrix), and totally disappeared at 130 °C. The poor thermal unstability makes the structure-directing action of the polymer matrix invalid. No special features were found on substrate after pyrolysis. Cross-linkage should be an efficient method targeting the stable film structure against solvents and heat annealing.[18] It has been reported that both PS and PAA could be effectively cross-linked under deep UV irradiation in certain conditions, though the mechanism was not clear. The well accepted photochemical cross-linking mechanism for PS is stated below[19] and drawn in the Supporting Information, Scheme 1. By abstracting hydrogen atoms from polymer molecules, macroradicals are formed during the irradiation. The movement of polymer macromolecules in the solid state is restricted, but free radicals can migrate along the polymer chain until they are trapped by other free radicals or by impurities. When two macroradicals are close to each other, the cross-linking may occur. This technique has been further developed to fabricate nanoporous functional polymeric films by selectively cross-linking the PS matrix and degrading a poly(methyl methacrylate) (PMMA) minority in a PS-*b*-PMMA diblock copolymer.[20] As for PAA, either chain scission or cross-linking reaction occurs simultaneously under UV irradiation, accompanied with the formation of anhydride.[19] Deep UV irradiation not only effectively cross-links the polymer matrix but also facilitates the preservation of honeycomb structures,[13−15] which is an indispensable step for the formation of regular inorganic patterns on substrate as discussed below. After 4 h UV cross-linking, the 3D honeycomb structures in PSPAA film could withstand temperatures up to 320 °C, an increase of more than 200 K as compared to the non-cross-linked films.[13] The top-view and cross-section view of the microporous PSPAA/APTES hybrid film after 4 h UV irradiation are shown in images e and f in Figure 2, respectively. Both the honeycomb pattern and spatial structures in the hybrid film are highly maintained without collapse after photochemical cross-linking.

The structure-directing action of the cross-linked polymer matrix is explained as the following. After UV irradiation, the thermal stability of PSPAA was significantly improved. The thermal decomposition rate of cross-linked polymer was slowed down because of the prohibited unzipping and depropagation processes,[21] as revealed by the TG results (Figure 3a). The char yield of the cross-linked PSPAA was 35% even heated up

(18) Kabuto, T.; Hashimoto, Y.; Karthaus, O. *Adv. Funct. Mater.* **2007**, *17*, 3569.
(19) Rånby, B.; Rabek, J. F. *Photodegradation, Photooxidation and Photostabilizationof Polymers*; Wiley: New York, 1975.
(20) (a) Thurn-Albrecht, T.; Schotter, J.; Kästle, G. A.; Emley, N.; Shibauchi, T.; Krusin-Elbaum, L.; Guarini, K.; Black, C. T.; Tuominen, M. T.; Russell, T. P. *Science* **2000**, *290*, 2126. (b) Thurn-Albrecht, T.; Steiner, R.; DeRouchey, J.; Stafford, C. M.; Huang, E.; Bal, M.; Tuominen, M.; Hawker, C. J.; Russell, T. P. *Adv. Mater.* **2000**, *12*, 787. (c) Yang, S. Y.; Ryu, I.; Kim, H. Y.; Kim, J. K.; Jang, S. K.; Russell, T. P. *Adv. Mater.* **2006**, *18*, 709.
(21) Levchik, G. F.; Si, K.; Levchik, S. V.; Camino, G.; Wilkie, C. A. *Polym. Degrad. Stab.* **1999**, *65*, 395.

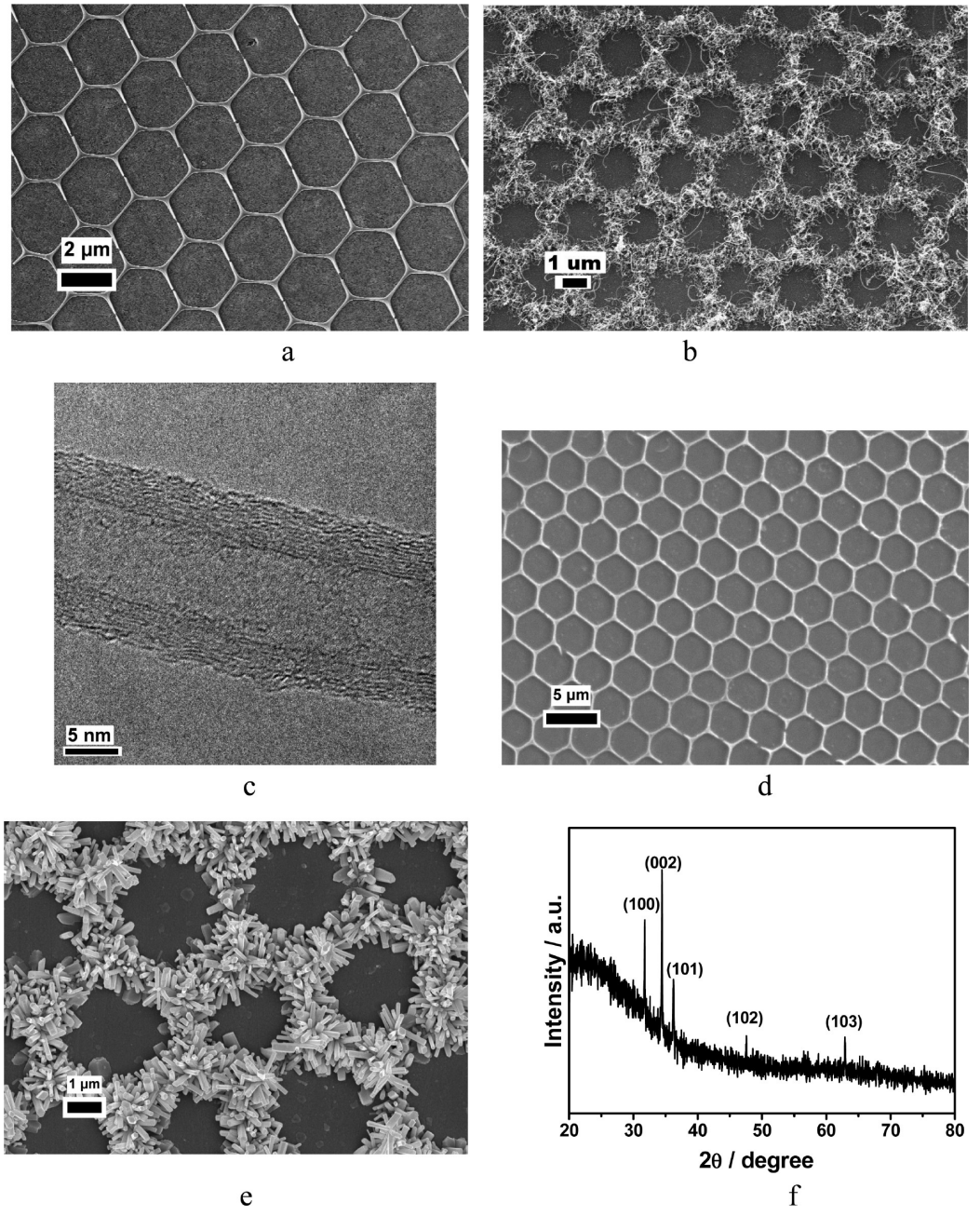

Figure 4. (a) SEM image of honeycomb structured ferrous pattern on Si substrate after UV irradiation and pyrolysis. (b) SEM image of carbon nanotubes arrays grown on honeycomb structured ferrous pattern. (c) High-resolution TEM image of the obtained carbon nanotubes. (d) SEM image of honeycomb structured ZnO pattern on Si substrate after UV irradiation and pyrolysis. (e) SEM image of hydrothermal ZnO nanorod arrays grown on honeycomb structured ZnO pattern. (f) X-ray diffraction pattern of the as-grown ZnO nanorod arrays on glass substrate.

to 450 °C at a rate of 5 °C/min in an air atmosphere. It took another 5 h annealing for the complete decomposition of the remained polymer at this temperature. APTES is a well-known silica precursor, as reported in many literatures.[22] In addition, the conversion rate of APETS into silica in air is accelerated once temperature more than 200 °C.[23] It is reasonable to speculate that the skeleton of the polymer microporous film is gradually replaced by the pyrolytic products of the incorporated APTES during the pyrolysis. Eventually, silica micropatterns are formed. A piece of cross-linked PSPAA/APTES microporous film supported on glass substrate was pyrolyzed according to the procedures mentioned in the Experimental Section. XPS analysis suggests that the atomic concentration of carbon is around zero and the silicon/oxygen ratio is close to 1:2 after 5 h holding at 450 °C in air (see the Supporting Information, Figure S2). This result then implies that the polymer matrix has been totally decomposed and APETS has been successfully converted into silica. The rainbow color on glass substrate (Figure 3b) is a clear proof that highly ordered silica patterns were created after pyrolysis

(22) (a) Son, M.; Ha, Y.; Choi, M. C.; Lee, T.; Han, D.; Han, S.; Ha, C. S. *Eur. Polym. J.* **2008**, *44*, 2236. (b) Wu, C. L.; Zheng, J. S.; Huang, C. B.; Lai, J. P.; Li, S. Y.; Chen, C.; Zhao, Y. B. *Angew. Chem., Int. Ed.* **2007**, *46*, 5393. (c) Ek, S.; Iiskola, E. I.; Niinisto, L. *Langmuir* **2003**, *19*, 3461.

(23) Hashem, K. M. E. *Appl. Surf. Sci.* **2003**, *217*, 302.

process. Microscopy observations (Figure 3c and 3d) reveal that the walls of the obtained silica micropatterns become thinner and sharper, suggesting that much materials was burned off. The micropatterns have the identical spacing and size with that of the micropores on the as-prepared film surface, indicative of the in situ formation of inorganic patterns on the honeycomb structures. Even after a long ultrasonic rinse with organic solvents. the silica patterns were found tightly bound to the substrate.

The versatility of this fabrication process is demonstrated by preparing ordered patterns with different chemical species on various solid substrates, simply through the choice of functional precursors. Furthermore, we are able to grow CNT and ZnO nanorod arrays taking advantage of the functionalized inorganic patterns, without the need of expensive and complicated lithographic procedure.[24]

Casting from a PSPAA/ferrocene (the precursor of Fe) CS_2 solution with a concentration of 15 mg mL^{-1}, a honeycomb patterns on silicon wafer was prepared after the same UV exposure and pyrolysis process as mentioned above (Figure 4a). The XPS spectra of PSPAA/ferrocene after pyrolysis on Pt film are shown in the Supporting Information, Figures S3 and S4. Either carbon or oxygen or iron peak was found. The core scan of Fe definitely shown that the incorporated ferrocene has been partially oxidized. Upon H_2 treatment, the ferrous composition was reduced and became activated, which initiated the growth of CNTs. The selective growth of honeycomb CNT arrays on the hexagonal edges (Figure 4b) is explained as the follows. During the pyrolysis, the trench bottom sunk down on substrate, and then stable $FeSi_2$ and Fe_2SiO_4 particles were formed due to chemical reactions between silicon surface and Fe particles at high temperature, leading to an inhibition of nanotube growth in the Si regions.[25] However, the ferrous composition on the hexagonal edges was isolated from the substrate and could be reduced to initial the growth of CNTs array. The formed CNTs are multiwalled tubes having an average diameter of 8 nm, confirmed by high-resolution transmission electron microscopy and shown in Figure 4c. The fabrication of ZnO nanorod arrays starts from the preparation of ZnO honeycomb pattern by using $Zn(acct)_2$ as the functional precursor [Supporting Information, Figure S5]. $Zn(acct)_2$ was converted into ZnO and formed the skeleton of the patterns after pyrolysis, as shown in Figure 4d. Then hydrothermal ZnO growth was carried out by suspending the patterned substrate upside-down in an open crystallizing dish filled with an aqueous solution of zinc nitrate hydrate and methenamine or diethylenetriamine at 90 °C.[26] The substrate was put facedown to keep any precipitates from falling down onto the substrate from the solution body, which would otherwise inhibit the growth of the desired nanostructures or possibly initiate secondary growth.[27] A typical synthesis (3 h) yielded rods with diameters ranging from 90 to 200 nm and length of 2−3 μm (Figure 4e). The average size of the rods increased with longer reaction time, up to 500 nm wide by 5 μm long for a 9 h experiment, whereas the honeycomb patterns were preserved. The crystal structure of the as-grown ZnO nanorods was examined by X-ray diffraction (XRD) pattern. The scanning results of the sample are shown in Figure 4f, where the main peaks have been labeled indicating a typical wurtzite structure.[28] No efforts have been made to optimize the growth of ZnO rods and the control of high aspect ratio. In the future, modified techniques will be used to address the issues.

Conclusion

In summary, we have developed a facile and versatile method to prepare highly ordered inorganic patterns on solid substrates by pyrolyzing cross-linked polymer/functional precursor hybrid films. UV cross-linking effectively improves the thermal stability of polymer matrix, which plays an important role in the structure-directing action. The inorganic micropatterns are functionalized to create CNT and ZnO nanorod arrays by simply changing different precursors. This simple technique offers new prospects in the field of micropatterns, nanolithography and template. More micropatterns with other chemical species and their template application are currently under investigation.

Acknowledgment. L.L. gratefully acknowledges the National Natural Science Foundation of China (50703032 and 20974089), the Natural Science Foundation of Fujian Province (2009J06029), and the Program for New Century Excellent Talents of Ministry of Education of China.

Supporting Information Available: Additional figures (PDF). This material is available free of charge via the Internet at http://pubs.acs.org.

(24) (a) Xu, S.; Ding, Y.; Wei, Y. G.; Fang, H.; Shen, Y.; Sood, A. K.; Polla, D. L.; Wang, Z. L. *J. Am. Chem. Soc.* **2009**, *131*, 6670. (b) Xu, S.; Wei, Y.; Kirkham, M.; Liu, J.; Mai, W.; Davidovic, D.; Snyder, R. L.; Wang, Z. L. *J. Am. Chem. Soc.* **2008**, *130*, 14958. (c) Haeffner, M.; Heeren, A.; Haug, A.; Schuster, E.; Sagar, A.; Fleischer, M.; Peisert, H.; Burghard, M.; Chasse, T.; Kern, D. P. *J. Vac. Sci. Technol., B* **2008**, *26*, 2447. (d) Lu, J.; Yuan, D. N.; Liu, J.; Leng, W. N.; Kopley, T. E. *Nano Lett.* **2008**, *8*, 3325.
(25) Jung, Y. J.; Wei, B. Q.; Vajtai, R.; Ajayan, P. M. *Nano Lett.* **2003**, *3*, 61.
(26) (a) Greene, L. E.; Law, M.; Goldberger, J.; Kim, F.; Johnson, J. C.; Zhang, Y. F.; Saykally, R. J.; Yang, P. D. *Angew. Chem., Int. Ed.* **2003**, *42*, 3031. (b) Pacholski, C.; Kornowski, A.; Weller, H. *Angew. Chem., Int. Ed.* **2002**, *41*, 1188.
(27) Wang, Z. L. *ACS Nano* **2008**, *2*, 1987.
(28) Greyson, E. C.; Babayan, Y.; Odom, T. W. *Adv. Mater.* **2004**, *16*, 1348.